AGU PUBLICATIONS

Geophysical Research Letters

RESEARCH LETTER
10.1002/2017GL074538

Key Points:
- Regular sampling of the Florida Current since 1982 resolves spatial patterns of salinity and velocity and decadal changes thereof
- North Atlantic water contributes as much or more volume transport and salinity anomaly transport as South Atlantic water
- All subsurface waters salinified between 1982–1987 and 2001–2015 and caused a 3% net increase in salinity anomaly transport

Supporting Information:
- Supporting Information S1

Correspondence to:
Z. B. Szuts,
zszuts@apl.washington.edu

Citation:
Szuts, Z. B., & Meinen, C. S. (2017). Florida Current salinity and salinity transport: Mean and decadal changes. *Geophysical Research Letters*, *44*, 10,495–10,503. https://doi.org/10.1002/2017GL074538

Received 12 JUN 2017
Accepted 30 SEP 2017
Accepted article online 9 OCT 2017
Published online 21 OCT 2017

Florida Current Salinity and Salinity Transport: Mean and Decadal Changes

Zoltan B. Szuts[1] and **Christopher S. Meinen**[2]

[1]Applied Physics Lab, University of Washington, Seattle, WA, USA, [2]NOAA Atlantic Oceanographic and Meteorological Lab, Miami, FL, USA

Abstract The Florida Current (FC) contributes to Atlantic circulation by carrying the western boundary flow of the subtropical gyre and the upper branch of meridional overturning circulation. Repeated FC hydrographic (velocity, salinity, and temperature) sections during 1982–1987 and 2001–2015 characterize its water mass structure and associated transport variability. On average, FC volume transport comes from subtropical North Atlantic water (NAW, 44%), Antarctic Intermediate Water (AAIW, 14%), surface water (SW, 27%), and an indistinct source (Rem 15%), while salinity transport relative to the average salinity along 26°N comes from NAW (55%), AAIW (0.2%), SW (30%), and Rem (15%). From 1982–1987 to 2001–2015, NAW, AAIW, and Rem salinified by 0.03–0.16 g kg^{-1} and increased the salinity anomaly transport by 3%. These patterns imply that advective salt transport by the FC (1) is sensitive to subtropical North Atlantic variability and (2) is partially decoupled from the volumetric pathway of the upper overturning branch.

Plain Language Summary Surface currents in the Atlantic Ocean flow northward as part of a global overturning circulation. Overturning transports heat and salt to northern latitudes as a major contribution to global climate. At 26°N in the Atlantic, almost all the northward flow is carried by the Florida Current (FC). This study uses temperature and salinity measurements of the FC in 1982–1987 and 2001–2015 to interpret what sets northward salt transport and how it changes over two decades. Below the surface, the FC has become much saltier by 0.05–0.01 g/kg. The net northward salt transport has increased by 3%, a small but significant amount. Though changes in volume transport have the potential for causing large changes in salt transport, the observations show instead that increased salt transport is driven primarily by saltier waters from the subtropical North Atlantic. FC salt transport appears to be partially decoupled from volume transport associated with overturning. These results provide evidence that changing stratification associated with saltier subtropical water does lead to changes to oceanic advection of salt on a basin scale.

1. Background

The Florida Current (FC) carries flows associated with two major circulation systems, the Atlantic meridional overturning circulation (AMOC) and the subtropical gyre. Whereas the AMOC is a global system that transports large amounts of heat and salt northward in the subtropical North Atlantic (e.g., Stammer et al., 2003), the subtropical gyre is a regional pattern driven by winds whose import is thought to be more local. Variabilities of these circulation patterns, and their associated fluxes of heat and salt or freshwater, have significant impact on the Atlantic Ocean and beyond (e.g., Vellinga & Wood, 2002). To understand and attribute FC variations to dynamics of the AMOC or the subtropical gyre, it is crucial that FC temperature and salinity patterns be characterized in a systematic and robust manner.

Together, temperature and salinity define water masses that spread from formation regions along circulation pathways. Past studies (Schmitz & Richardson, 1991, hereafter SR91; Schmitz et al., 1993) concluded that relatively fresh waters from the South Atlantic form the upper AMOC branch that transits from the equator to the FC (Johns et al., 2002). It does not necessarily follow, however, that this fresh water is the dominant control on northward salt transport by the FC. In fact, basin-wide northward salt flux is positively correlated with AMOC strength (McDonagh et al., 2015), because the northward flowing FC is much saltier than the deep southward flow in the interior Atlantic. By contrast, the subtropical gyre imports fresh water northward to balance evaporation over the gyre center. This means that a water parcel in the FC could carry either salt or freshwater northward, depending on its pathway. Insight from the past decade of AMOC studies has not previously been applied to interpret the water mass constituents of the FC. In particular, recent studies of both the cold lower and warm upper limbs of the AMOC further north have been shown to be less continuous than anticipated

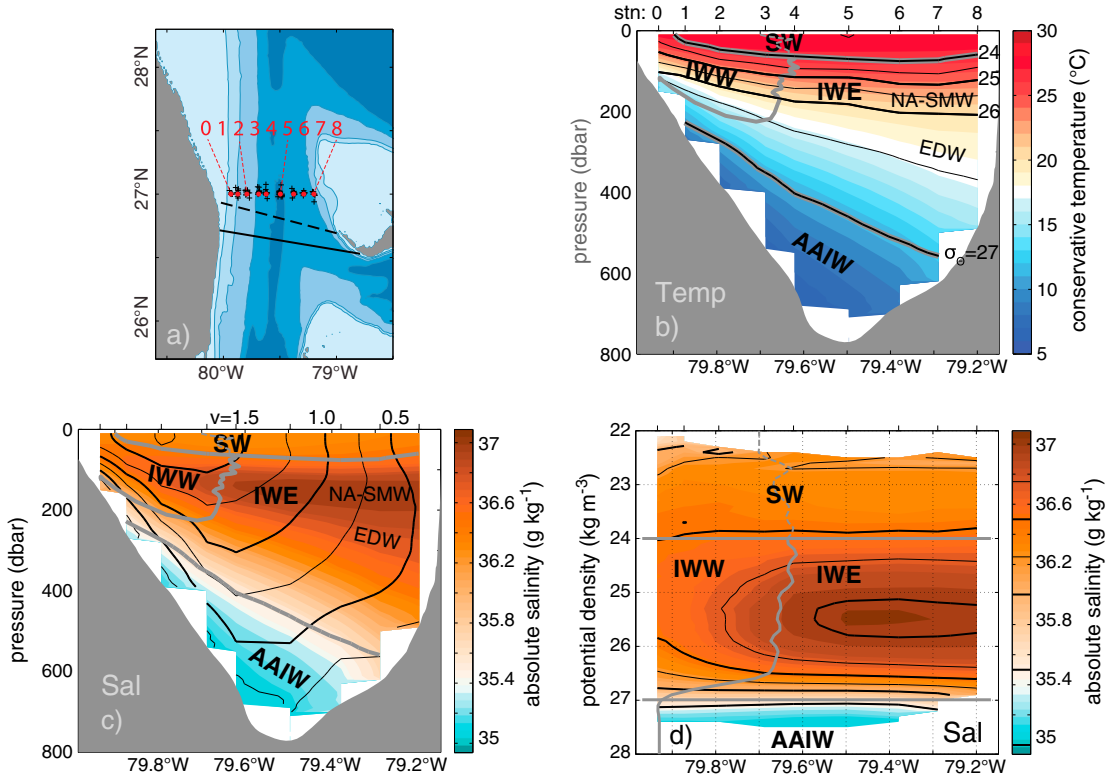

Figure 1. (a) The Straits of Florida, showing nominal station locations (red dots, labeled with station numbers), actual positions of the CTD/LADCP profiles (black crosses), the location of the historic cable (dashed black), and the current cable (solid black). Bathymetric contours are at 100, 250, 500, and 750 m (Smith and Sandwell, 1997). Isopycnal average sections from NOAA/AOML CTD/LADCP data 2001–2015. (b) Average temperature versus depth, with potential density contours (black lines, in kg m^{-3}) and station positions labeled at top. (c) Average salinity versus depth, with velocity contours (black lines, in m s^{-1}). (d) Average salinity versus potential density, with black lines for clarity (thick every 0.5 g kg^{-1}, thin at 36.25 and 36.75 g kg^{-1}). The salinity color scale of Figures 1c and 1d is set to white at the interior average salinity (S_0 = 35.338 g kg^{-1}, see text). Figures 1b–1d also show the station locations at top, the dividing lines between water mass classes (thick grey lines) at potential densities of 24 and 27 g kg^{-1} and the Ertel's potential vorticity front, labels for four water mass classes (surface water, SW; intermediate water west, IWW; intermediate water east, IWE; and Antarctic Intermediate Water, AAIW), and the core locations of two distinct water masses within the IWE class, eighteen-degree water (EDW) and North Atlantic salinity maximum water (NA-SMW).

(Bower et al., 2009; Foukal & Lozier, 2016). The implication of significant interior pathways and boundary-interior interactions raises the possibility of significant modification by mixing. The fundamental question of what controls salt or heat throughput by the AMOC cannot be answered without analyzing the FC.

This study addresses these questions by using measurements of velocity, salinity, and temperature in the FC, from the 1980s to the present, to evaluate water mass properties and transports of volume and salinity. Quantifying the contributions by water masses to the FC transports provides new insights on advective-diffusive pathways for the time-averaged flow and for decadal adjustments.

2. Data and Methods

We analyze three different data sets, each consisting of full-depth profiles at nine common stations across the Straits of Florida at 27°N (Figure 1).

Hydrographic profiles from 1982 to 1987 were collected with a Neil Brown conductivity, temperature, and depth (CTD) profiler during 11 cruises (e.g., Molinari et al., 1985, see also the supporting information). There are 9–11 profiles for most stations, except for 5 at station 0 and 19 at station 5. Measurement accuracies are 0.01°C and 0.003–0.005 practical salinity unit (psu) (e.g., Ratnaswamy et al., 1985) for all cruises, except for the first three which had lower salinity accuracy (0.01–0.02 psu).

Velocity profiles from 1982 to 1986 were sampled with a Pegasus profiler (Spain et al., 1981), which measures velocity to within 0.01 m/s by acoustic ranging from sound sources on the seafloor. We compensate for high

correlation between measurements collected close together in time by using the integral timescale (Emery and Thompson, 1997) Γ = 19 days calculated from 20 years of daily FC cable transports (Meinen et al., 2010). Profiles collected within 2Γ (Emery & Thomson, 1997; Meinen et al., 2009) contribute less than a full degree of freedom (DOF) to the average; for example, three profiles within 38 days collectively provide only 2 DOF. From the total of ~65 Pegasus transects collected in the 1980s (see Figure S1 in the supporting information), there are 24–26 DOF at most stations (station 0 has 15 DOF). Note that Pegasus and CTD profiles in the 1980s were not collected simultaneously. The fact that velocity sampling ended 1 year before hydrographic sampling ended has minimal impact on our analysis of average fields, because of the high level of subannual variability in the FC.

Routine hydrography/velocity transects (2001–2015) were initiated in 2001 and have been sustained to the present by NOAA/Atlantic Oceanographic and Meteorological Laboratory (AOML) (Garcia & Meinen, 2014; Meinen & Luther, 2016; Szuts & Meinen, 2013), using a Seabird CTD and a Teledyne RDI LADCP (Lowered Acoustic Doppler Current Profiler) sampling system. Transects are collected 3–4 times per year, and each represents a single DOF as the sections are always more than 2Γ apart in time. The seasonal cycle is well sampled over 15 years (Szuts & Meinen, 2013; see the supporting information). There are 55 transects through July 2015. Accuracies are 0.001°C, 0.003 psu (Hooper & Baringer, 2014), and 3.7 cm/s (Garcia & Meinen, 2014).

All hydrographic data are converted into TEOS-10 units (Intergovernmental Oceanographic Commission, Scientific Committee on Oceanic Research, and International Association for Physical Sciences of the Oceans, 2010). The hydrographic and velocity data sets are averaged into a composite, referred to as 1982–1987 or into 2001–2015, to reduce synoptic variability and to focus on low-frequency patterns. Averages are calculated in density layers to preserve water mass properties.

The sections are gridded onto a uniform cross section following Szuts and Meinen (2013). A fixed cross section is required for consistent volume transport between data sets. Reasonable choices for extrapolating to the bottom and side boundaries lead to average differences of 0.5–1 sverdrup (Sv) for volume transport (Baringer & Larsen, 2001; Szuts & Meinen, 2013). Volume and salinity anomaly transport are calculated as

$$T_{\mathrm{vol}} = \iint v\, dx\mathrm{d}z \quad , \qquad T_{\mathrm{sal0}} = \iint (S - S_0) v\, dx\mathrm{d}z \tag{1}$$

where v is meridional velocity, S is salinity, and S_0 is a constant reference salinity. Temperature transport is calculated (see the supporting information) but not presented, because it is of limited use to evaluate water origins. The reference salinity S_0 is the area average across the Atlantic at 26°N calculated by McDonagh et al., 2015 from Argo profiles and deep mooring data. We convert their value to TEOS-10 for use here, S_0 = 35.338 g kg^{-1}.

This type of referencing is used to calculate transport or fluxes for temperature or salinity (e.g., Johns et al., 2011; McDonagh et al., 2015; Szuts & Meinen, 2013). It simplifies trans-basin integrals by decomposing the section into an area-averaged constant, a zonally averaged profile, and the residual (Hall & Bryden, 1982; Wijffels et al., 1996). Across the Atlantic at 26°N (McDonagh et al., 2015), the average salinity relates to the throughflow transport, the anomaly relative to the average salinity relates to the vertical circulation (overturning), and the anomaly relative to zonal profile relates to the horizontal circulation (i.e., gyre circulation). These definitions match the concept of the AMOC as vertical circulation and the gyre as horizontal circulation, even though both patterns have zonal and vertical expressions across the transect.

Our results depend on careful analysis of statistical confidence. The uncertainty of composite averages is the standard error of the mean (SEM) calculated over all transects in the data set. The significance of differences of composite averages is evaluated with Welch's t test (at 95% confidence), which accounts of unequal DOFs and variances between composites. The SEM cannot be calculated for quantities involving salinity and velocity in the 1980s, however, because these measurements were not collected simultaneously. Covariance between velocity and salinity is high because the FC is dominantly geostrophic (Johns & Schott, 1987; Szuts & Meinen, 2013). The CTD/LADCP data set is used to assess the importance of unresolved covariance in the 1980s (see the supporting information). Covariance does not affect average T_{sal}, which can be calculated two ways: (1) calculated for each transect and then averaged (Table S2 in the supporting information) or (2) calculated by multiplying composite-averaged velocity and salinity fields (Table 1). The results agree within 5%, and we present results from the second method to maintain internal consistency. Covariance is dominant for SEM of absolute salinity transport, and so no uncertainty is shown for 1982–1987 (Table 1). Results from

Table 1
Transports in Water Mass Classes

		Volume transport (Sv)	Salinity transport (Sv g kg^{-1})	Salinity anomaly transport (Sv g kg^{-1})	Transport-weighted salinity anomaly (g kg^{-1})
SW	1980s	8.5 ± 0.4	308	8.96 ± 0.34*	1.06 ± 0.07*
	2000s	9.2 ± 0.3	334 ± 12	9.68 ± 0.38	1.05 ± 0.05
	diff	0.7	26	0.72	−0.006
IWW		4.9 ± 0.3	178	5.23 ± 0.25*	1.07 ± 0.09*
		4.0 ± 0.2	146 ± 7	4.59 ± 0.23	1.15 ± 0.06
		−0.9	−32	−0.64	0.08
IWE		14.8 ± 0.5	539	17.37 ± 0.51*	1.18 ± 0.06*
		14.8 ± 0.2	540 ± 9	18.11 ± 0.30	1.23 ± 0.05
		0.0	1	0.74	0.05
AAIW		4.5 ± 0.3	158	−0.08 ± 0.06*	−0.017 ± 0.013*
		4.6 ± 0.2	162 ± 6	0.07 ± 0.06	0.016 ± 0.014
		0.1	4	0.15	0.034
Total		32.6	1183	31.49	0.97
		32.5 ± 0.4	1182 ± 16	32.46 ± 0.41	1.00 ± 0.01
		−0.1	−1	0.97	0.031

Note. The three values in each cell are (top) the 1982–1987 average, (middle) the 2001–2015 average, and (bottom) the difference (2001–2015 minus 1982–1987). The water masses are surface water (SW), intermediate water east (IWE) and intermediate water west (IWW), and Antarctic Intermediate Water (AAIW). Confidence limits are the statistical standard errors of the means, unless the value is marked with an asterisk (*) in which case the confidence limit was estimated via error propagation. The salinity reference is S_0 = 35.338 g kg^{-1}.

propagating uncertainty (Taylor, 1996) associated with salinity anomaly give uncertainties (Table 1, columns 3 and 4) that are comparable to the SEM uncertainties for 2001–2015 calculations (Table 1).

Transports are binned into four water mass classes for interpretation (Figure 1b): surface water (SW, $\sigma_\Theta < 24$ kg m^{-3}); middepth water, which we denominate intermediate water (IW, $24 < \sigma_\Theta < 27$ kg m^{-3}) and divide below into east and west; and Antarctic Intermediate Water (AAIW, $\sigma_\Theta > 27$ kg m^{-3}). Our definitions in TEOS-10 units are comparable to prior definitions from SR91 and Rhein et al. (2005).

The division of IW into east (IWE) and west (IWW) is defined relative to the front of Ertel's potential vorticity (EPV). Bower et al. (1985) described how a strong EPV gradient in the center of the Gulf Stream inhibits cross-stream mixing because EPV is conserved in free-flowing currents. In the Florida Current, we define the front (Figures 1b–1d, thick gray line) as the longitude where EPV gradients along isopycnals are 5×10^{-14} s^{-1} m^{-2} (Beal et al., 2006; Bower & Lozier, 1994). The front separates weakly stratified IW on the eastern side from highly stratified IW on the western side. The EPV calculation is revisited in the discussion. We expect that unresolved along-stream gradients contribute little to EPV in the FC, because their reported influence further downstream in the Gulf Stream at 38°N is small (<10%; Meinen & Luther, 2016).

3. Results

3.1. Average Water Mass Structure (2001–2015)

The composite-averaged structure of the FC (Figure 1) has small uncertainty because of the many DOFs. The associated variability (see the supporting information) is essential to calculate confidence limits on transports. Earlier studies (SR91; Rhein et al., 2005; McDonagh et al., 2015) relied on far fewer transects.

The deepest water mass class found in the strait, AAIW, is cold and fresh, reflecting its formation in the Southern Ocean. Eastern middepth water, IWE, demonstrates its subtropical origin by a salty signature. Two well-defined subtype water masses are located within the IWE class and contribute to its thickness: Salinity maximum water (SMW), which forms by evaporation within the subtropical gyre and spreads southwestward under the surface layer (e.g., Schmitt & Blair, 2015), and eighteen-degree water (EDW), which forms at the southern flank of the Gulf Stream and circulates around the gyre (e.g., Billheimer & Talley, 2013). In contrast to IWE, IWW is smoothly stratified vertically in salt and temperature and is a relatively thin layer. There is no consensus on the source of IWW, with proposed but unconfirmed origins including the tropical or South

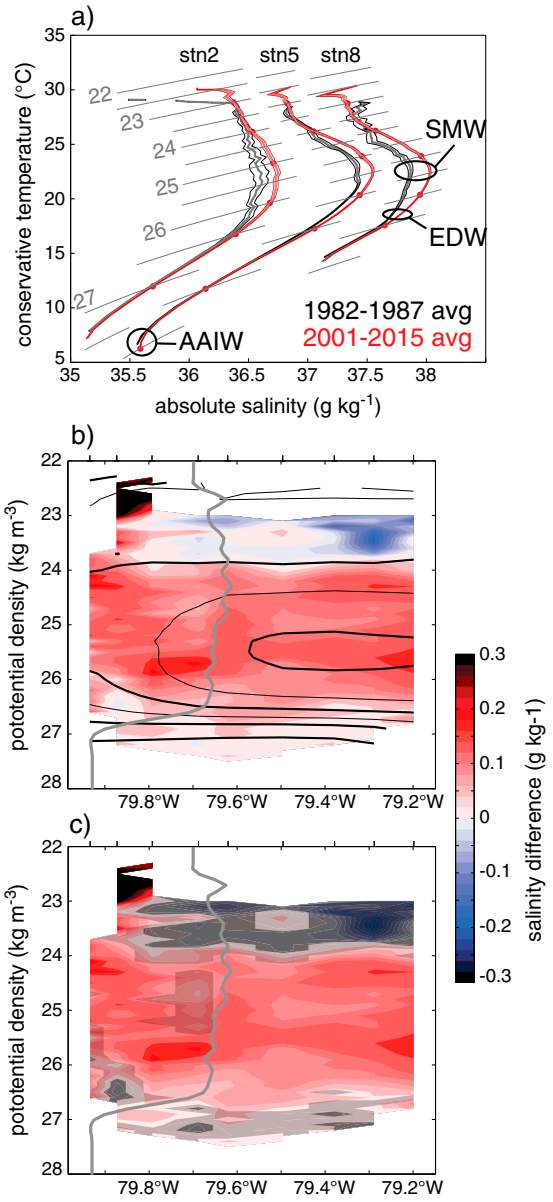

Figure 2. (a) Temperature/salinity diagram with the isopycnal average from 1982 to 1987 (thick gray, with thin black showing standard error of the mean) and from 2001 to 2015 (thick light red, with thin dark red showing standard error of the mean—note that the standard error lines sometimes overlap the average lines). See Figure 1a for station locations. Density sections of changes for the 2001–2015 average minus the 1982–1987 average. (b) Salinity change (color) and 2001–2015 average salinity (black lines every 0.5 g kg^{-1}). (c) Salinity change (color) and its statistical significance: significant (larger than Welch's *t* statistic) is unshaded; not significant but larger than the standard error of the mean is shaded light gray, and less than the standard error shaded dark gray. Also shown in Figures 2b and 2c is the EPV front (thick grey) and station positions at top.

Atlantic (Rhein et al., 2005), the Gulf of Mexico (Schmitz & McCartney, 1993), or the Caribbean (Schmidt et al., 2004). The surface layer, SW, is warm and moderately fresh, and warms and cools seasonally (Szuts & Meinen, 2013) in response to surface fluxes.

3.2. Average Transports (2001–2015)

Volume transport for 2001–2015 (Table 1) is unequally divided by the location of the EPV front with more transport in the east, either within IW (4.1 Sv for IWW, 14.7 Sv for IWE) or for all densities combined (9.4 Sv west of the EPV front, 23.1 Sv east). This asymmetry is a result of the highly stratified western region being relatively shallow and narrow compared to the region east of the front, even though the western region contains the surface velocity maximum. Transport of salt (where salt content is salinity times density) and temperature largely depends on volume transport (Johns et al., 2011; McDonagh et al., 2015; Szuts & Meinen, 2013). In essence, the more volume transport, the more salt and heat are carried. The water mass contribution to the total mean volume and salinity transports are the same: IWE 46%, SW 28%, IWW 12%, and AAIW 14%. Our section-average total transports summing all water classes agree with previous estimates for net volume and salt transports (32.1 ± 3.3 Sv, Meinen et al., 2010; 1143 ± 98 Sv psu, McDonagh et al., 2015; mean ± standard deviation).

Salinity anomaly transport is used so we can estimate the fraction of FC salinity transport that participates in basin-wide salt flux. Our section-average total salinity anomaly transport, 32.46 Sv g kg^{-1}, is within 15% of the net salt flux carried by the Florida Current for basin-wide fluxes (27.4 Sv g kg^{-1}, calculated from McDonagh et al., 2015). The total salinity anomaly transport (Table 1, column 3) is composed of IWE 56%, SW 29%, IWW 15%, and AAIW 0.2%. The transport-weighted salinity anomaly (Table 1, column 4) estimates the excess salinity normalized by transport that a water mass contributes to salt balance across 26°N: IWW is saltiest, IWE and SW are slightly less salty, and AAIW has essentially zero anomaly.

3.3. Water Mass Changes, 2001–2015 Minus 1982–1987

Changes between 1982–1987 and 2001–2015 show increased salinity at all densities greater than 24 g kg^{-1}, seen in T/S space (Figure 2a) for the upper layers, and in density space (Figure 2c) for deeper layers. Diagnosing salinity changes on isopycnals must be done carefully, however. For example, consider the hypothetical case of a section of the T/S curve with positive slope that warms with no change in salinity. The curve rises vertically in T/S space, but, on constant isopycnals, there is apparent freshening and cooling. As a result, we must identify unambiguous changes of temperature and salinity at vertical positions defined independently of density or depth. There are three such locations in the FC:

1. The SMW core, defined as the salinity maximum at station 8, salinified by 0.16 ± 0.02 g kg^{-1} (95% *t* test confidence). This salinity maximum is likely a remnant of downward mixing of salty water from the center of the gyre into the top of the thermocline. It is not a traditional water mass because it results from mixing.
2. The EDW core, defined by a stratification minimum at station 8, has become deeper (by 30 m), colder (by 0.5°C), and slightly fresher (by 0.04 g kg^{-1}). When a property feature changes depth, there is no change in water mass structure if the salinity change equals the vertical displacement times the vertical salinity gradient (and same for temperature). For the EDW core, the observed cooling equals that caused by a 30 m descent against the negative vertical gradient of temperature. For salinity, the observed change is saltier

by 0.04 g kg^{-1} than that caused by the vertical descent. Thus, EDW has not changed temperature but has become saltier.

3. AAIW is defined by a salinity minimum near 27.4 kg m^{-3}. Though the Straits of Florida at 27°N are too shallow to show the underside of the AAIW salinity minimum as seen in the interior basin (e.g., Bryden et al., 1996; Talley et al., 2011), a nearby salinity inflection is suggested at the bottom of station 5 by the steepening T/S curve. The hydrography in the 1980s and the 2000s was collected to a similar height above the bottom, and the deepest common density (27.4 kg m^{-3}) sampled in the 1980s and after 2000 has not changed depth. Thus, we conclude that the saltier bottom water reflects salinification of the deep AAIW by 0.03 ± 0.01 g kg^{-1} (95% *t* test confidence).

Because these three water masses have become saltier, it is likely that adjacent regions have also salinified. Accurately diagnosing intervening layers requires analyzing layer thickness and vertical motion of isopycnals. Though important to diagnose upstream changes, such details are beyond the scope of our study and are unnecessary to evaluate FC salinity transport.

Overall, all subsurface regions have become distinctly saltier on isopycnals (Figures 2c and 2d), with the largest and most robust increases in the upper IWE. Salinification has occurred both in the middepth salty IWE and in the deep fresh AAIW. The existing data sources cannot distinguish whether this salinification is caused by changes in source water properties or by changes in mixing fractions. There are no distinct water mass characteristics to evaluate in IWW, and we do not discuss SW because our isopycnal analysis is inappropriate for the atmosphere-forced surface mixed layer (e.g., Szuts & Meinen, 2013).

3.4. Transport Changes, 2001–2015 Minus 1982–1987

We find that total transports of volume and salinity by the FC have not changed between these two time periods. This is consistent with Meinen et al. (2010), who found no change in daily cable volume transport estimates since 1982; recall our earlier assessment that salinity transport is driven by volume transport. Salinity anomaly transport through the straits has increased by 3% over this period, a small but significant increase. Subannual variability of the AMOC volume transport, clearly evident in continuous moored array observations (e.g., Frajka-Williams et al., 2016), is not resolved by our data sets and is minimized by our use of composite averaging.

In terms of water mass classes, over this ~20 year span volume and salinity transports (Table 1) were redistributed from IWW to SW, with insignificant changes for other water masses. Salinification alone explains the observed increase in salinity anomaly transport from both IWE and AAIW, which together provide most (90%) of the net increase. Though AAIW contributes little to salinity anomaly transport, its contribution has changed sign from negative to positive. The remaining net increase (10%) comes from the redistribution of volume transport from IWW to SW, which mostly cancels for net salinity anomaly transport.

4. Discussion

These results provide insight into the structure of the AMOC volume and salt transport in the FC. The water mass analysis of SR91 concluded that surface and near-bottom waters in the FC originate in the southern hemisphere and provide 13 Sv to overturning (the accepted AMOC value in the early 1990s). Though our analysis finds similar transport of AAIW and SW (14 Sv), recent publications raise significant inconsistencies with SR91: (1) continuous monitoring finds a stronger AMOC of 17 Sv, (2) surface water pathways suggest that it does not leave the subtropical gyre (Brambilla & Talley, 2006), and (3) SR91 ignores strong horizontal gradients between IWE and IWW.

Identifying the AMOC component of the FC transport requires some preliminary assumptions:

1. The basin-wide northward transport across 26°N is the sum of overturning and gyre, which produces the flow of the FC (32.1 ± 3.3 Sv; Meinen et al., 2010) plus the Antilles Current (average of 1.3 Sv; Johns et al., 2011).
2. Following the framework of Kanzow et al. (2007), meridional transport across 26°N is divided into overturning (17.2 ± 5.6 Sv; McCarthy et al., 2012) and horizontal (gyre) circulation (the remainder, 16.2 Sv), with any mass-compensated interior flow being unresolved, such as from eddies or uncharacterized mean flows.
3. The northward upper AMOC branch is predominantly carried by the FC. Johns et al. (2002) show that this is accurate for flow through the Caribbean, but there is less clarity for the subsurface exchange from 26°N to the subpolar gyre.

4. The FC structure determines the downstream path.

The last point assumes that ocean mixing has limited impact on where a water parcel goes. The opposite extreme is overwhelming mixing—equal probability of any water mass parcel following any pathway. The real ocean falls between these two extremes, most likely with mixing playing a small but unclear role in large-scale circulation.

Now we consider which water masses can provide the 17 Sv needed for AMOC across 26°N. Each water mass is assessed based on whether it can exit the subtropical gyre.

1. IWW is the most likely to exit the subtropical gyre because it is west of the EPV front that acts as a barrier to free exchange (Bower et al., 1985).
2. AAIW is deeper than the EPV front and thus is unconstrained by it. Bottom friction leads to westward transport and upwelling, a potential mechanism to drive cross-front transport. Although synoptic measurements in the Straits found a convergent boundary layer generated by bottom friction (Seim et al., 1999), it is too weak to transport much volume: 1 Sv if active along the entire Straits of Florida (600 km).
3. SW, unlike deeper waters, is driven more by winds than by geostrophy. Downstream of the FC, westerlies drive Ekman transport into the subtropics. Almost no surface drifters deployed in the FC or Gulf Stream enter the subpolar gyre (Brambilla & Talley, 2006), and numerical trajectories and observed sea surface temperature confirm this lack of surface connectivity (Foukal & Lozier, 2016). Note that surface fluxes continually modify SW properties, so advective SW transport does not reflect water origins.
4. IWE can interact with the western side through horizontal eddies or isopycnal mixing, or with the bottom layer via shear stress. Horizontal shear includes transfer of negative potential vorticity from side boundary friction, as needed to balance the northward path of the FC across f/h contours.

The most likely contributor to AMOC is IWW (4.0 Sv), followed by AAIW beneath the dynamical EPV boundary (4.6 Sv). This only explains half of AMOC transport. Even if SW west of EPV contributes to AMOC, this only adds 5 Sv to explain 13.6 Sv total. A similar magnitude (13.8 Sv) is obtained by applying SR91's conclusion that FC AMOC comes from AAIW and all SW. The results of Brambilla and Talley (2006) and Foukal and Lozier (2016), however, strongly suggest that SW contributes little to AMOC. In any case, at least 3 Sv of AMOC remains unaccounted for.

Though the EPV front does separate salty IWE from fresh IWW, it does not divide transport in a way consistent with known AMOC strength. The EPV calculation assumes quasi-geostrophy with no friction (Beal et al., 2006), an incorrect assumption in the Florida Straits where boundary friction decreases effective PV in the frictional layer (Haynes & McIntyre, 1987). Frictional effects extend eastward and upward from the sloping western seafloor and would act to push the friction-corrected front eastward.

The only other water class that can supply the 3 Sv deficit is IWE. IWE could contribute as little as 3 Sv to AMOC, based on the two cases above, or, more likely, up to 9 Sv if SW contributes nothing to the AMOC. The IWE contribution is less certain than for other water mass classes because it is estimated as the remainder. Any increase in IWE contribution is equivalent to shifting the effective E/W dividing line of IW eastward.

Despite the qualitative nature of this argument, it is apparent that North Atlantic waters contribute directly to AMOC volume transport. Clear sources to AMOC are the South Atlantic (AAIW, 23%) and the North Atlantic (IWE, 17–52%), with the rest (25–60%) originating from indistinct regional mixing (IWW) or regional surface fluxes (SW). In other words, waters with properties set most recently in the North Atlantic supply roughly as much AMOC flow as South Atlantic waters, and potentially twice as much. If an intermediate level of isopycnal mixing is assumed, the same conclusion is reached by ascribing fractional AMOC contributions farther east.

For salinity anomaly transport, the percent contribution of North Atlantic waters (56%) is larger than for volume transport (46%), while there is practically no direct South Atlantic contribution (from AAIW). Both IW and SW reflect processes in the subtropics: IWW for regional mixing, IWE for evaporation over the gyre, and SW for air-sea fluxes in the subtropics and Caribbean including river input. Dividing FC salinity anomaly transport into AMOC and gyre contributions is difficult, because each circulation has different return salinities. The two circulations partially cancel across 26°N, as the AMOC carries salt northward and the gyre carries salt southward (McDonagh et al., 2015). More quantitative analysis requires data from the basin interior (e.g., Xu et al., 2016).

From our data, decadal changes of salinity anomaly transport depend more on salinity changes than on changes in volume transport. The transport-weighted salinity anomaly has increased for all subsurface water masses. The increases for IWE and IWW are not significant, while that for AAIW is significant and changes the sign of its contribution. The salinification of IWE and AAIW, which have no change in volume transport, explains 90% of the increase in total salinity anomaly transport (75% from IWW, 15% from AAIW; Table 1). When volume is redistributed, such as from IWW to SW, then the impact on salinity transport depends on the transport-weighted salinities. Because IWW and SW have similar transport-weighted salinity anomalies, their volume transfer largely cancels for salinity anomaly transport (−65% and 74%; from Table 1).

The decadal salinity changes described here result ultimately from surface fluxes. Saltier IWE, SMW, and EDW are consistent with increased subtropical evaporation, a manifestation of a stronger global hydrologic cycle (Durack & Wijffels, 2010). A stronger hydrologic cycle produces fresher AAIW at its origin in a region of high precipitation (e.g., Hutchinson et al., 2016). In contrast, at 27°N AAIW has a decadal trend of salinification. This implies that AAIW preferentially gains salt from subtropical regions as it flows north. The monotonic salinification of all subsurface water in the FC also suggests a diffusive source of salt from the subtropics.

Our finding that the water mass structure in the Florida Current helps set the northward transport of salinity anomaly has implications for observing future changes of North Atlantic circulation. The existing AMOC monitoring network (e.g., Smeed et al., 2014) uses cable voltages to resolve the FC volume transport. To observe any geostrophic adjustments of the upper AMOC branch, it is necessary to continue measuring temperature and salinity in the FC. The impact of diffusive modification of water masses that we infer happens upstream will also happen downstream from the Straits of Florida. If regional mixing has a similar magnitude in the subpolar North Atlantic, then the downstream importance of FC salt transport is reduced. Instead, storage and release of heat and salt by volume transport (Evans et al., 2017; Kelly et al., 2016; McCarthy et al., 2015) may dominate fluxes on the basin scale. In any case, salt transport by the FC is sensitive to processes in the subtropical North Atlantic, which suggests that AMOC volume transport and FC salt transport are partially decoupled at this location.

Acknowledgments
The 1980 CTD data were obtained from the World Ocean Database (Boyer et al., 2009); CTD/LADCP transects are funded by NOAA CPO-OOMD (FundRef 100007298, Western Boundary Time Series project) with additional support from NOAA/AOML and are available from http://www.aoml.noaa.gov/phod/wbts/. We thank Andrey Shcherbina for helpful discussions, and two anonymous reviewers for constructive comments. Z.B.S. was supported by NSF-1356383. C.S.M. was supported by NOAA/CPO-OOMD and NOAA-AOML.

References

Baringer, M. O., & Larsen, J. C. (2001). Sixteen years of Florida Current transport at 27°N. *Geophysical Research Letters*, *28*, 3179–3182. https://doi.org/10.1029/2001GL013246

Beal, L. M., Chereskin, T. K., Lenn, Y. D., & Elipot, S. (2006). The sources and mixing characteristics of the Agulhas Current. *Journal of Physical Oceanography*, *36*, 2060–2074.

Billheimer, S., & Talley, L. D. (2013). Near cessation of eighteen degree water renewal in the western North Atlantic in the warm winter of 2011–2012. *Journal of Geophysical Research: Oceans*, *118*, 6838–6853. https://doi.org/10.1002/2013JC009024

Bower, A. S., & Lozier, M. S. (1994). A closer look at particle exchange in the Gulf Stream. *Journal of Physical Oceanography*, *24*, 1399–1418.

Bower, A. S., Lozier, M. S., Gary, S. F., & Böning, C. W. (2009). Interior pathways of the North Atlantic meridional overturning circulation. *Nature*, *459*, 243–247.

Bower, A. S., Rossby, H. T., & Lillibridge, H. L. (1985). The Gulf Stream | barrier or blender? *Journal of Physical Oceanography*, *15*, 24–32.

Boyer, T. P., Antonov, J. I., Baranova, O. K., Garcia, H. E., Johnson, D. R., Locarnini, R. A., … Zweng, M. M. (2009). *World Ocean Database 2009. NOAA Atlas NESDIS 66*. Washington, DC: U.S. Government Printing Office.

Brambilla, E., & Talley, L. D. (2006). Surface drifter exchange between the North Atlantic subtropical and subpolar gyres. *Journal of Geophysical Research*, *111*, C07026. https://doi.org/10.1029/2005JC003146

Bryden, H. L., Griffiths, M. J., Lavin, A. M., Millard, R. C., Parrilla, G., & Smethie, W. M. (1996). Decadal changes in water mass charateristics at 24N in the subtropical North Atlantic Ocean. *Journal of Climate*, *9*, 3162–3186.

Durack, P. J., & Wijffels, S. E. (2010). Fifty-year trends in global ocean salinities and their relationship to broad-scale warming. *Journal of Physical Oceanography*, *23*, 4342–4362. https://doi.org/10.1175/2010JCLI3377.1

Emery, W. J., & Thomson, R. E. (1997). *Data Analysis Methods in Physical Oceanography*, (1st ed., 634 pp.). Pergamon, Oxford, UK: Elsevier Science Ltd.

Evans, D. G., Toole, J., Forget, G., Zika, J. D., Naveira Garabato, A. C., Nurser, A. J. G., & Yu, L. L. (2017). Recent wind-driven variability in Atlantic water mass distribution and meridional overturning circulation. *Journal of Physical Oceanography*, *47*, 633–647. https://doi.org/10.1175/JPO-D-16-0089.1

Foukal, N. P., & Lozier, M. S. (2016). No inter-gyre pathway for sea-surface temperature anomalies in the North Atlantic. *Nature Communications*, *7*, 11333. https://doi.org/10.1038/ncomms11333

Frajka-Williams, E., Meinen, C. S., Johns, W. E., Smeed, D. A., Duchez, A., Lawrence, A. J., … Rayner, D. (2016). Compensation between meridional flow components of the Atlantic MOC at 26°N. *Ocean Science*, *12*(2), 481–493.

Garcia, R. F., & Meinen, C. S. (2014). Accuracy of Florida Current volume transport measurements at 27°N using multiple observational techniques. *Journal of Atmospheric and Oceanic Technology*, *31*, 1169–1180. https://doi.org/10.1175/JTECH-D-13-00148.1

Hall, M. M., & Bryden, H. L. (1982). Direct estimates and mechanisms of ocean heat transport. *Deep Sea Research*, *29*(3), 339–359.

Haynes, P. H., & McIntyre, M. E. (1987). On the evolution of vorticity and potential vorticity in the presence of diabatic heating and frictional or other forces. *Journal of the Atmospheric Sciences*, *44*(5), 828–841. https://doi.org/10.1175/1520-0469(1987)044%3C0828:OTEOVA%3E2.0.CO;2

Hooper, J. A. V., & Baringer, M. O. (2014). Hydrographic measurements collected aboard the UNOLS ship R/V Walton smith, 2014: Western boundary time series cruise: Florida current, NOAA Data Report OAR AOML 50, NOAA Atlantic Oceanographic and Meteorological Laboratory, Miami, FL. https://doi.org/10.7289/V5JD4TSZ

Hutchinson, K., Swart, S., Meijers, A., Ansorge, I., & Speich, S. (2016). Decadal-scale thermohaline variability in the Atlantic sector of the Southern Ocean. *Journal of Geophysical Research: Oceans*, *121*, 3171–3189. https://doi.org/10.1002/2015JC011491

Intergovernmental Oceanographic Commission, Scientific Committee on Oceanic Research, and International Association for Physical Sciences of the Oceans (2010). The international thermodynamic equation of seawater - 2010: Calculation and use of thermodynamic properties. Manuals and guides 56, Intergovernmental Oceanographic Commission.

Johns, W. E., Baringer, M. O., Beal, L. M., Cunningham, S. A., Kanzow, T., Bryden, H. L., … Curry, R. (2011). Continuous estimate of Atlantic oceanic freshwater flux at 26°N. *Journal of Climate*, *24*(10), 2429–2449. https://doi.org/10.1175/2010JCLI3997.1

Johns, W. E., & Schott, F. A. (1987). Meandering and transport variations of the Florida current. *Journal of Physical Oceanography*, *17*, 1128–1147.

Johns, W. E., Townsend, T. L., Fratantoni, D. M., & Wilson, W. D. (2002). On the Atlantic inflow to the Caribbean Sea. *Deep-Sea Research Part I*, *49*, 211–243.

Kanzow, T., Cunningham, S. A., Rayner, D., Hirschi, J. J.-M., Johns, W. E., Baringer, M. O., … Marotzke, J. (2007). Observed flow compensation associated with the MOC at 26.5°N in the Atlantic. *Science*, *317*(5840), 938–941. https://doi.org/10.1126/science.1141293

Kelly, K. A., Drushka, K., Thompson, L., Le Bars, D., & McDonagh, E. L. (2016). Impact of slowdown of Atlantic overturning circulation on heat and freshwater transports. *Geophysical Research Letters*, *43*, 7625–7631. https://doi.org/10.1002/2016GL069789

McCarthy, G., Frajka-Williams, E., Johns, W. E., Baringer, M. O., Meinen, C. S., Bryden, H. L., … Cunningham, S. A. (2012). Observed interannual variability of the Atlantic meridional overturning circulation at 26.5°N. *Geophysical Research Letters*, *39*, L19609. https://doi.org/10.1029/2012GL052933

McCarthy, G. D., Haigh, I. D., Hirschi, J. J.-M., Grist, J. P., & Smeed, D. A. (2015). Ocean impact on decadal Atlantic climate variability revealed by sea-level observations. *Nature*, *521*, 508–510. https://doi.org/10.1038/nature14491

McDonagh, E., King, B. A., Bryden, H. L., Courtois, P., Szuts, Z. B., Baringer, M. O., … McCarthy, G. (2015). Continuous estimate of Atlantic oceanic freshwater flux at 26°N. *Journal of Climate*, *28*, 8888–8906. https://doi.org/10.1175/JCLI-D-14-00519.1

Meinen, C. S., Baringer, M. O., & Garcia, R. F. (2010). Florida Current transport variability: An analysis of annual and longer-period signals. *Deep-Sea Research Part I*, *57*(7), 835–846. https://doi.org/10.1016/j.dsr.2010.04.001

Meinen, C. S., & Luther, D. S. (2016). Structure, transport and vertical coherence of the Gulf Stream from the Straits of Florida to the Southeast Newfoundland Ridge. *Deep-Sea Research Part I*, *111*, 16–33. https://doi.org/10.1016/j.dsr.2016.02.002

Meinen, C. S., Luther, D. S., & Baringer, M. O. (2009). Structure, transport and potential vorticity of the Gulf Stream at 68°W: Revisiting older data sets with new techniques. *Deep Sea Research*, *56*, 41–60. https://doi.org/10.1016/j.dsr.2008.07.010

Molinari, R. M., Maul, G. A., Chew, F., Wilson, W. D., Busheell, M., Mayer, D., … Sanford, T. B. (1985). Subtropical Atlantic climate studies: Introduction. *Science*, *227*, 292–295.

Ratnaswamy, M. J., Wilson, D., & Molinari, R. L. (1985). Current velocity and hydrographic observations in the Straits of Florida: Subtropical Atlantic Climate Studies (STACS), 1983 and 1984, NOAA Data Report ERL AOML 5, Miami, FL.

Rhein, M., Kirchner, K., Mertens, C., Steinfeldt, R., Walter, M., & Fleischmann-Wischnath, U. (2005). Transport of South Atlantic water through the passages south of Guadeloupe and across 16°N, 2000–2004. *Deep-Sea Research Part II*, *52*, 2234–2249. https://doi.org/10.1016/j.dsr.2005.08.003

Schmidt, M. W., Spero, H. J., & Lea, D. W. (2004). Links between salinity variation in the Caribbean and North Atlantic thermohaline circulation. *Nature*, *428*, 160–163. https://doi.org/10.1038/nature02346

Schmitt, R. W., & Blair, A. (2015). A river of salt. *Oceanography*, (1), 40–45. https://doi.org/10.5670/oceanog.2015.04

Schmitz, W. J. Jr., Luyten, J. R., & Schmitt, R. W. (1993). On the Florida Current T/S envelope. *Bulletin of Marine Science*, *53*(3), 1048–1065.

Schmitz, W. J. Jr., & McCartney, M. S. (1993). On the North Atlantic circulation. *Reviews of Geophysics*, *31*, 29–49. https://doi.org/10.1029/92RG02583

Schmitz, W. J. Jr., & Richardson, P. L. (1991). On the sources of the Florida current. *Deep Sea Research*, *38*(supp 1), S379–S409.

Seim, H. E., Winkel, D. P., Gawarkiewicz, G. G., & Gregg, M. C. (1999). A benthic front in the Straits of Florida and its relationship to the structure of the Florida Current. *Journal of Physical Oceanography*, *29*, 3125–3132.

Smeed, D. A., McCarthy, G. D., Cunningham, S. A., Frajka-Williams, E., Rayner, D., Johns, W. E., … Bryden, H. L. (2014). Observed decline of the Atlantic meridional overturning circulation 2004–2012. *Ocean Science*, *10*, 29–38. https://doi.org/10.5194/os-10-29-2014

Spain, P., Dorson, D., & Rossby, T. H. (1981). PEGASUS: A simple, acoustically tracked, velocity profiler. *Deep Sea Research*, *28A*, 1553–1567.

Stammer, D., Wunsch, C., Giering, R., Eckert, C., Heimbach, P., Marotzke, J., Adcroft, A., Hill, C. N., & Marshall, J. (2003). Volume, heat, and freshwater transports of the global ocean circulation 1993–2000, estimated from a general circulation model constrained by World Ocean Circulation Experiment (WOCE) data, *Journal of Geophysical Research*, *108*(C1), 3007. https://doi.org/10.1029/2001JC001115

Szuts, Z. B., & Meinen, C. S. (2013). Salinity transport in the Florida Straits. *Journal of Atmospheric and Oceanic Technology*, *30*(5), 971–983. https://doi.org/10.1175/JTECH-D-12-00133.1

Talley, L. D., Pickard, G. L., Emery, W. J., & Swift, J. H. (2011). *Descriptive physical oceanography: An introduction*, (6th ed., p. 555). London, UK: Academic Press, Elsevier.

Taylor, J. R. (1996). *An introduction to error analysis: The Study of uncertainties in physical measurements*, (2nd ed.). Sausalito, CA: University Science Books.

Vellinga, M., & Wood, R. A. (2002). Global climate impacts of a collapse of the Atlantic thermohaline circulation. *Climatic Change*, *54*, 729–742.

Wijffels, S. E., Toole, J. M., Bryden, H. L., Fine, R. A., Jenkins, W. J., & Bullister, J. L. (1996). The water masses and circulation at 10°N in the Pacific. *Deep-Sea Research Part Part I*, *43*(4), 501–544.

Wilburn, A. M., Johns, E., & Bushnell, M. (1987a). Current velocity and hydrographic observations in the Straits of Florida, the Caribbean Sea and offshore of the Antillean Archipelago: Subtropical Atlantic Climate Studies (STACS), 1984 and 1985. NOAA Data Report ERL AOML 8, Atlantic Oceanographic and Meteorological Laboratory, Miami, FL.

Wilburn, A. M., Johns, E., & Bushnell, M. (1987b). Current velocity and hydrographic observations in the Straits of Florida, the Caribbean Sea and offshore of the Antillean Archipelago: Subtropical Atlantic Climate Studies (STACS), 1986. NOAA Data Report ERL AOML 10, Atlantic Oceanographic and Meteorological Laboratory, Miami, Florida.

Wilburn, A. M., Johns, E., & Bushnell, M. (1998). Current velocity and hydrographic observations in the southwestern North Atlantic ocean: Subtropical Atlantic Climate Studies (STACS), 1987. NOAA Data Report ERL AOML 12, Atlantic Oceanographic and Meteorological Laboratory, Miami, Florida.

Xu, X., Rhines, P. B., & Chassignet, E. P. (2016). Temperature-salinity structure of the North Atlantic circulation and associated heat and freshwater transports. *Journal of Climate*, *29*(21), 7723–7742.